

## **Impact of 2015–2016 ENSO on the winter bloom and associated phytoplankton community shift in the northeastern Arabian Sea**

**P. J. Vidya<sup>1,2\*</sup> and Siby Kurian<sup>1</sup>**

<sup>1</sup>CSIR- National Institute of Oceanography, Dona Paula, Goa-403 004, India.

<sup>2</sup>Present address: National Centre for Antarctic and Ocean Research, Headland Sada, Goa-403 804, India.

\*Corresponding author Email: [pjvidya@gmail.com](mailto:pjvidya@gmail.com)

### **Abstract**

The present study explores the impact of 2015-16 El-Niño Southern Oscillation (ENSO) on the winter phytoplankton bloom in the northeastern Arabian Sea (NEAS). *In situ* Chlorophyll *a* (Chl*a*) from the bio-Argo float (2013-2016) and phytoplankton pigment data collected onboard *R.V. Sindhu Sankalp* (February 2013 and 2016) have been used to decipher the 2015-2016 ENSO modulated variability. During a normal winter, convective mixing deepens the mixed layer (ML) and increases the availability of nutrients in the euphotic zone. During the 2015-16 ENSO, the intensity of the convection (evaporation) was weaker than normal and this, in turn, weakened the convective mixing in the following winter. However, during the 2015-16 ENSO event, a warm core eddy deepened the ML further by pushing the nutricline downwards, thereby reducing the availability of nutrients. Changes in the physical condition during the 2015-16 ENSO altered the nutrient availability which in turn affected the Chl*a* production and associated phytoplankton community structure. The Bio-Argo observations show 50 % reduction in Chl*a* during February 2016 compared to a normal year, which we attribute to the ENSO event of 2015-2016. Additionally, pigment data shows a reduction in the abundance of microplankton (diatoms and dinoflagellates) and an increase in abundance of picoplankton in the NEAS. Our results clearly indicate that 2015 ENSO played a dominant role in altering the phytoplankton community composition and in turn the productivity of the Arabian Sea.

**Key words:** ENSO, Winter Convection, Phytoplankton Pigments, Warm Core eddy, Mixed Layer Depth

### **Key Points:**

- ENSO weakens the intensity of convective cooling in the NEAS.
- Warm-core eddy controls the ML dynamics during the ENSO event.
- 2015-2016 ENSO event altered the phytoplankton community structure in the NEAS.

## 1. Introduction

The seasonal reversal of the surface winds, from the southwest during the summer and from the northeast during the winter, makes the Arabian Sea (AS) a unique region. On the one hand, the strong southwest monsoon winds during June to September associated with the low-level Findlater jet (Findlater, 1969), causes strong upwelling of cold and nutrient-rich subsurface water along the coast of Somalia and Oman, and comparatively weak upwelling along the eastern AS (Schott and McCreary, 2001). This upwelling leads to phytoplankton bloom during the summer (Banse, 1986; Brock et al., 1992). On the other hand, during the northeast monsoon (winter), the Eurasian continents cool, and a high-pressure region develops over the Tibetan Plateau. This results in cold and dry northeast monsoon winds (during November to February) and leads to net heat loss, causing evaporative cooling in the northern part of the AS (Dickey et al., 1998). It further leads to deepening of the Mixed Layer (ML) and upward entrainment of nutrients into the surface layers (Banse 1987; Madhupratap et al., 1996; Prasanna Kumar et al., 1996; Prasanna Kumar et al., 2001) from the base of the ML, fuelling a winter bloom. The operation of different physical processes during the summer and winter alter the vertical flux of nutrients and ML depth leading to strong seasonality in phytoplankton bloom during the summer and winter (Banse and English, 2000). The strong upwelling during the summer (July–September) (Banse, 1968, 1987; Wiggert et al., 2005; Levy et al., 2007; McCreary et al., 2009; Wiggert et al., 2009; Kone et al., 2009) and convective mixing during the winter (December–February) increase biological productivity (Madhupratap et al., 1996) in the Arabian Sea. These processes make the Arabian Sea one of the most productive regions in the world's oceans (Prakash and Ramesh, 2007).

Apart from the seasonal variations, the inter-annual variability of phytoplankton blooms were also addressed by several researchers (Banse and McClain, 1986; Banse and English, 1993; Bauer et al., 1991; Madhupratap et al., 1996; Gundersen et al., 1998; Prasanna Kumar et al., 2001; Wiggert et al., 2002; Sarma et al., 2006) using satellite-derived *Chl<sub>a</sub>*, as well as *in-situ* measurements. Prasanna Kumar et al. (2001) suggested that increase in convective mixing leads to the deepening of the ML and affects the *Chl<sub>a</sub>* bloom. Wiggert et al. (2002) documented that intensity of the inter-annual variations of the *Chl<sub>a</sub>* bloom was controlled by the thermocline variations. Keerthi et al. (2017) showed that in NEAS, ML controls the amplitude of the phytoplankton bloom on the inter-annual time scale. A modelling study by Vijith et al. (2016) documented that winter phytoplankton bloom in the NEAS is not only controlled by the convective deepening of the ML, but also by the West India Coastal Current (WICC). The current advects low-salinity water poleward during the winter and inhibits the deepening of the ML (Shankar et al., 2016). This, in turn, inhibits the nutrient

entrainment and affects the size-based distribution of small and large phytoplankton and their elemental composition.

The El Niño Southern Oscillation (ENSO) and Indian Ocean Dipole (IOD) are the most important climate modes that lead to inter-annual variability in the tropical Indian Ocean (Murtugudde et al., 2000). ENSO events are associated with a weakening of trade winds in the equatorial Pacific and lead to warming in the central and eastern Pacific and cooling in the western Pacific. Though it originates in the Pacific, it affects the global weather pattern (McPhaden et al., 2006). For example, ENSO warms the western Indian Ocean (Murtugudde and Busalacchi, 1999). Like ENSO in the Pacific, IOD originates in the tropical Indian Ocean and exhibits its own mode of inter-annual variability (Murtugudde and Busalacchi, 1999; Saji et al., 1999; Webster et al., 1999). Currie et al. (2013) showed that ENSO has more effect than the IOD on Chl $a$  variability in the AS.

Several researchers (e.g., Sawant and Madhupratap, 1996; Madhupratap et al., 1996; Tarran et al., 1999; Wood, 1999; Garrison et al., 2000) have addressed the role of seasonal reversal of winds on the phytoplankton community in the northern AS during the summer and winter monsoons. However, the linking of an ENSO event with the phytoplankton community in the NEAS has not yet been discussed. Here, we examine the impact of the 2015-16 ENSO on the variability of Chl $a$  and phytoplankton community in the NEAS during the winter (DJF) using bio-Argo data and *in situ* phytoplankton pigments.

## 2. Data and Methods

### 2.1 Satellite data

The monthly mean chlorophyll data was obtained from version 3.1 of the European Space Agency's Ocean Color-Climate Change Initiative (OC-CCI). The OC-CCI Chlorophyll product merges MERIS, Aqua-MODIS, SeaWiFS and VIIRS data (source: <http://www.esa-oceancolour-cci.org/>) with a spatial resolution of 4km x 4km. The vertical structure of temperature (monthly mean) was analysed for the period from January 2013 to December 2016 using gridded ARGO data. The data (1° x 1° resolution) was obtained from the INCOIS Live Access server (source: <http://las.incois.gov.in/las/>). Daily optimum interpolated (OI) AVHRR (Advanced Very High-Resolution Radiometer) sea surface temperature (SST) data (0.25° x 0.25°) for the period from 1 January 2013 to 31 December 2016 was taken from <http://coastwatch.pfeg.noaa.gov/erddap/griddap/>. Daily 1° x 1° gridded evaporation data for the same period was taken from Objectively Analysed air-sea Fluxes (OA fluxes; source: <http://oafux.whoi.edu>) and daily air temperature (2.5° x 2.5°) for the same period was downloaded from NCEP-Reanalysis

(<https://www.esrl.noaa.gov/psd/data/gridded/data.ncep.reanalysis2.html>). In order to investigate the meridional variations in evaporation, SST and air temperature, the data were averaged over the region 63°E–69°E from 17°N to 24°N during the following periods: December 2013–February 2014; December 2014–February 2015; and December 2015–February 2016.

The delayed time (DT) Sea Level Anomaly data (SLA) (0.25° x 0.25°) was obtained from the European Copernicus Marine Environment Monitoring Service (CMEMS). This product comprises data from all the altimeter missions: Jason-3, Sentinel-3A, HY-2A, Saral/AltiKa, Cryosat-2, Jason-2, Jason-1, T/P, ENVISAT, GFO and ERS1/2. It provides both near real-time (NRT) and delayed time mode (DT mode) data for oceanic studies. The delayed time daily SLA data are freely available at <http://marine.copernicus.eu/services-portfolio/access-to-products/>.

## **2.2 Bio-Argo data**

The vertical profiles of temperature and Chl*a* (real-time) were obtained from the Bio-Argo float (WMO ID-2902092). The Bio-Argo data were provided by the Biogeochemical Argo data management team ([biogeochemical-argo.org](http://biogeochemical-argo.org)) and are publically available in two modes (real-time and delayed mode). Real-time data was distributed in less than 24 hours and was quality controlled and flagged using an automated procedure. The delayed-mode data was produced after one year and required control and validation by a scientific expert. The temperature profiles were used to compute the Mixed Layer Depth (MLD) which is determined as the depth at which the temperature is 0.5°C lower than the surface value. The Chl*a* was measured based on the fluorescence sensor, and the accuracy is 0.015 mg m<sup>-3</sup> (Catherine et al., 2015). The float measures Chl*a* data during the ascending profile at a five day interval with depth ranging from 5m to 1200m. All the individual profiles were visually checked and linearly interpolated up to 200m. The quality control of the data was carried out based on Catherine et al. (2015) and is freely available at <ftp://ftp.ifremer.fr/ifremer/argo>.

## **2.3 Niño3.4 index**

To characterize the ENSO variability, we used the Niño3.4 index which was obtained from <http://stateoftheocean.osmc.noaa.gov/sur/ind/dmi.php>. The Niño3.4 index represents the SST anomalies in the equatorial Pacific (170°W–120°W and 5°N–5°S) (Trenberth, 1997). For the correlation analysis, we have used normalized Niño3.4 index from <https://www.ncdc.noaa.gov/teleconnections/enso/indicators/sst.php>. To understand the inter-annual variability contributed by ENSO in the AS, the normalized Niño3.4 index during October to December was correlated with the spatial pattern of Chl*a* during December-February\_(during

December of the same year and January and February of the following year). The significance of the correlation coefficients was calculated using a two-tailed t-test.

## 2.4 Phytoplankton pigment analysis

Water samples for phytoplankton pigments were collected at 17°N; 68°E (Arabian Sea Time Series site under the SIBER-INDIA project) in the NEAS during SSK-46 (February 2013) and SSK-87 (February 2016) cruises onboard *R.V. Sindhu Sankalp* during the northeast monsoon (NEM; Figure 1b). Water samples were collected at discrete depths (surface, 10, 25 and 50 m onboard SSK-46 and surface, 25, 55, 70 and 100 m onboard SSK-87) using Niskin bottles mounted on a rosette frame carrying a CTD (SeaBird) system. Samples for phytoplankton pigments were immediately filtered on GF/F filters (0.7µm, 25mm) under dark and cold conditions and preserved at -80°C until analysis. The frozen filters were extracted with 100% methanol and analyzed using HPLC (Agilent Technologies) using an Eclipse XDB C8 column. Pigments were separated using a binary solvent gradient (solvent A- 70/30: methanol /0.5 M ammonium acetate; solvent B- 100% methanol) as detailed in Kurian et al. (2012). The eluting pigments were detected at 450 and 665 nm by the diode array detector. Commercially available standards obtained from DHI Inc. (Denmark) were used for the identification and quantification of pigments including both chlorophylls and carotenoids. Identification of pigments was based on the retention time and also by visible spectra matching, and the response factor based on the standard run was used for quantification of samples. In the present study, we used seven pigments (Fucoxanthin, Peridinin, Alloxanthin, 19'-Hexanoyloxyfucoxanthin (19'HF), 19'-Butanoyloxyfucoxanthin (19'BF), Zeaxanthin and TChl*b* (Chl*b*+divinyl chlorophyll*b* (DivChl*b*)) as markers of phytoplankton taxa (diagnostic pigments; DP) as detailed in Uitz et al. (2006). Though having limitations, diagnostic indices are useful for representing the major groups contributing to the phytoplankton community according to the average size of the cell (micro-, nano- and pico-phytoplankton). Size fractionated contributions of phytoplankton ( $f_{micro}$ ,  $f_{nano}$ , and  $f_{pico}$ ) were calculated as follows:

$$f_{micro} \% = 100 \times (1.41 [\text{fucoxanthin}] + 1.41 [\text{peridinin}]) / \sum \text{DP} \quad (>20 \mu\text{m})$$

$$f_{nano} \% = 100 \times (0.60 [\text{alloxanthin}] + 0.35 [19'\text{BF}] + 1.27 [19'\text{HF}]) / \sum \text{DP} \quad (2 \text{ to } 20 \mu\text{m})$$

$$f_{pico} \% = 100 \times (0.86 [\text{zeaxanthin}] + 1.01 [\text{TChl}b]) / \sum \text{DP} \quad (<2 \mu\text{m})$$

## 3. Result and Discussions

To understand the relation between Chl*a* and ENSO, the normalized Niño3.4 index during October–December was correlated with satellite-derived Chl*a* during December–February of the following year. The negative correlation (-0.5) in the northern (north of 15°N) and western AS

suggests that *Chla* decreases during the ENSO year (Figure 1b). A positive correlation (0.5) observed in the northeastern part of the AS indicates that other factors may also influence the *Chla* variability, which is out of the scope of the present study. Figure 1a (Niño3.4 index) shows that ENSO-2015 was one of the strongest of its kind in the past four decades (1980–2016). Using the available time series (2013-2016) measurement of *Chla* from the Bio-Argo float, the present study explores the impact of the 2015 ENSO on the winter phytoplankton bloom in the NEAS. The following winters were chosen for a more detailed analysis: December 2013-February 2014; December 2014-February 2015 and December 2015-February 2016. Among these, the 2015-16 winter that followed the ENSO event of 2015 is considered an ENSO affected winter. Whereas, the 2013-14 and 2014-15 winters are considered normal.

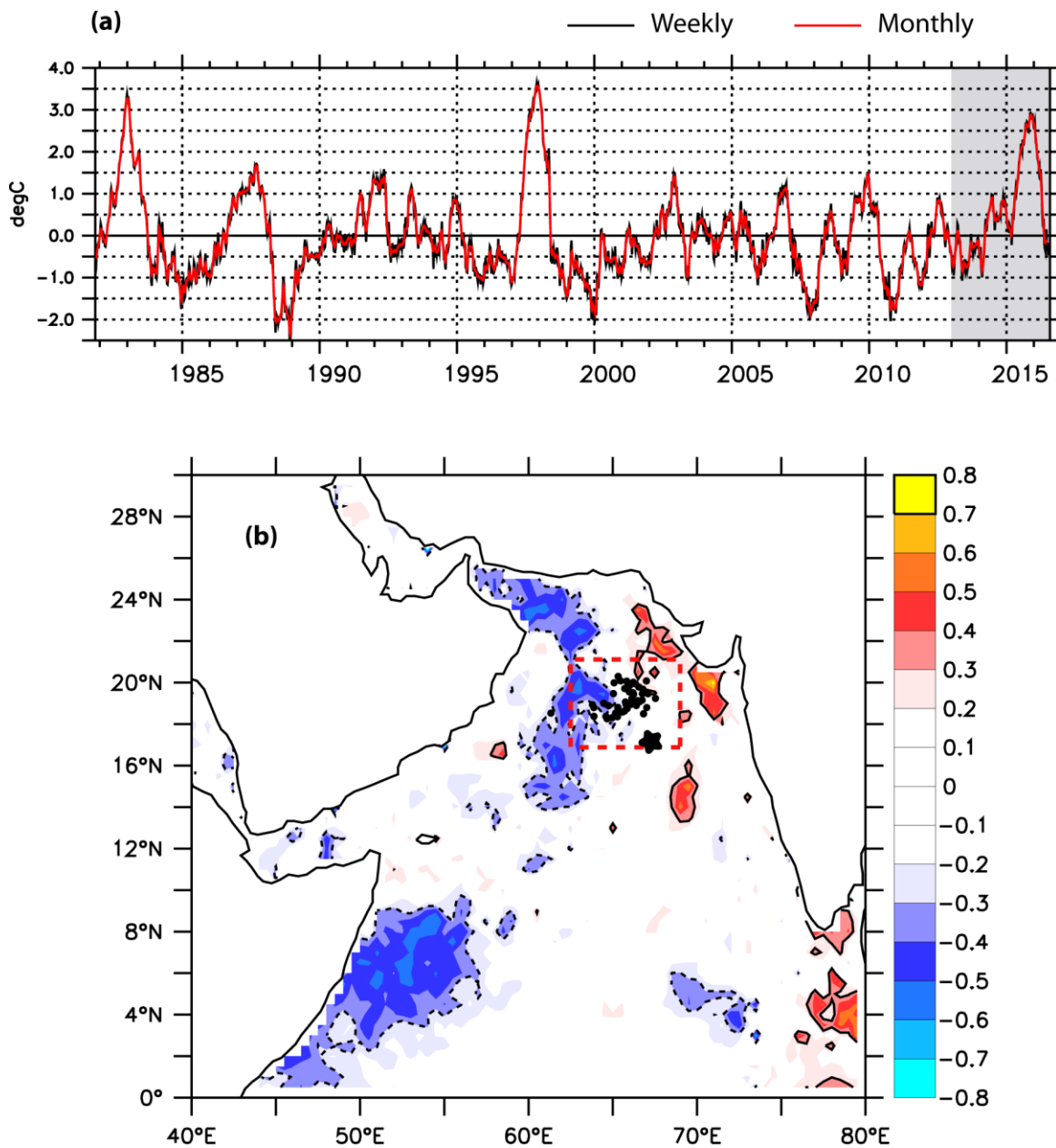


**Figure 1**(a) Time series of Niño3.4 index for the period 1981–2016; Black line represents the weekly mean Niño3.4 index, and the red line represents the monthly mean Niño3.4 index. (b) Correlation between normalized Niño3.4 index during October–December and satellite-derived Chl $a$  above 95% significant level (contours) during winter (DJF). The filled star indicates the location of water column sampling for phytoplankton pigments. The dashed red rectangle represents the winter convective region. Black solid circles represent the track of Bio-Argo float (WMO ID- 2902092).

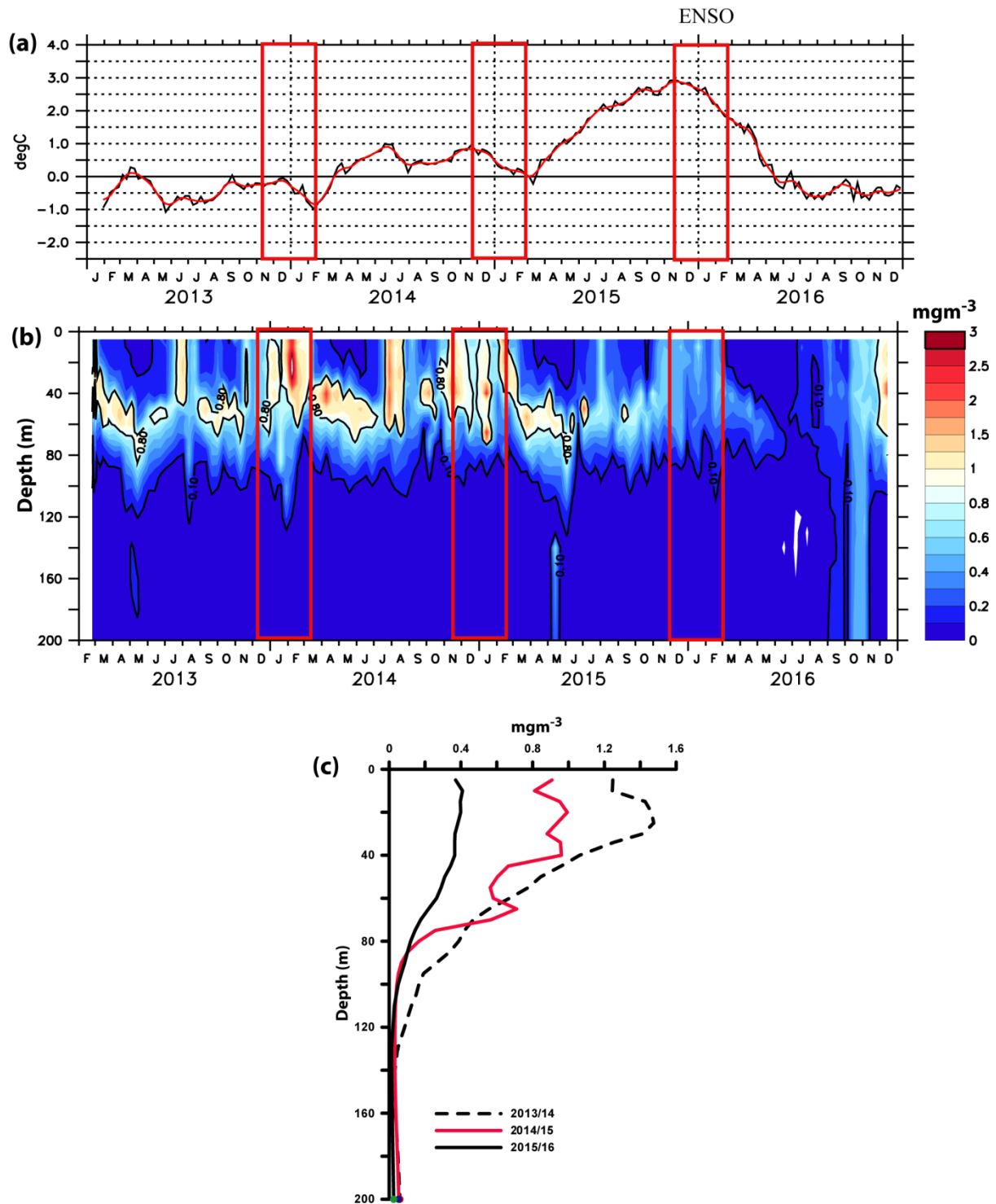


**Figure 2**(a) Time series of Niño3.4 index for the period 2013–2016. The black line represents the weekly mean Niño3.4 index, and the red line represents the monthly mean Niño3.4 index. (b) Temporal evolution of Chla from Bio-Argo float (WMO ID: 2902092) and (c) vertical profiles of Chla during December–February (averaged) of 2013–14; 2014–15 and 2015–16. The red boxes in the Figure 2a & 2b represent December–February.



Satellite sensor provides an estimate of *Chla* only in the first optical depth which is much shallower than the deep chlorophyll maxima (DCM) (Al-Niami et al., 2017). Hence, based on the satellite-derived *Chla* concentration, the ENSO impact on *Chla* in the euphotic zone was not possible until now. The advent of Bio-Argo floats in recent times has helped to resolve this issue. The vertical structure of *Chla* (from the Bio-Argo float) in the upper water column showed an increase in concentration from December to February, with peak values observed in February (except 2016; Figure 2b). The column-integrated *Chla* in the upper 200m was 71.5  $\text{mgm}^{-2}$ , 59.3  $\text{mgm}^{-2}$  and 29.8  $\text{mgm}^{-2}$  during the winters (DJF) of 2013–14, 2014–15 and 2015–16 respectively. This is consistent with the vertical profiles of *Chla* (Figure 2c) which also showed a minimum value during 2015-16 winter (solid black line); whereas the maximum was during 2013-14 (dashed black line). Very low *Chla* (29.8  $\text{mgm}^{-3}$ ) in the upper 200m during the 2015–16 winter was assumed to be controlled by the 2015 ENSO. The ENSO-modulated *Chla* variability in the AS has been reported earlier using data collected prior to 2012 (Currie et al., 2013; Keerthi et al., 2017). Our study, however, focusses on the impact of 2015 ENSO on the *Chla* biomass and also the associated phytoplankton community shift in the AS. The observed variability in *Chla* during the 2015-16 winter was further explored using both atmospheric and oceanic parameters.

Evaporation, SST, air temperature, surface wind speed and mixed layer depth during the winters (DJF) of 2013–14, 2014–15 and 2015–16 (Figure 3a-e) were analysed to understand the impact of the 2015-16 ENSO. The cool, dry northeast wind increases the evaporation in the NEAS and is directly related to the strength of the winter convection. Evaporation was the highest during 2013–14, followed by 2014–15, and lowest during 2015–16 (Figure 3a). Unlike evaporation, SST (Figure 3b) and air temperature (Figure 3c) were lowest during 2013–14, followed by 2014–15, and highest during 2015–16. Wind speed was lowest during 2015-16 (ENSO event) and highest during 2014-15 (Figure 3d). Though wind speed was high during 2014-15, the corresponding ML deepening was lowest (Figure 3e) in that year, which needs to be explored further. The strong evaporation during the winter leads to net heat loss and densification of the upper water column, which further initiates the convective cooling and deepening of the ML (Madhupratap et al., 1996). The minimum wind speed during the 2015-16 ENSO event was enhanced by the weakening of the winter monsoon winds (Murtugude et al. 1999), which further led to the reduction in evaporation, increase in SST (which leads to the stratification of the water column) and weakening of the convective cooling. The reduction in convective cooling may alter the intensity of the ML deepening (and inhibit vertical mixing) and nutrient supply to the euphotic zone. This, in turn, reduces the availability of nutrients in the euphotic zone and further alters the phytoplankton biomass (*Chla*).

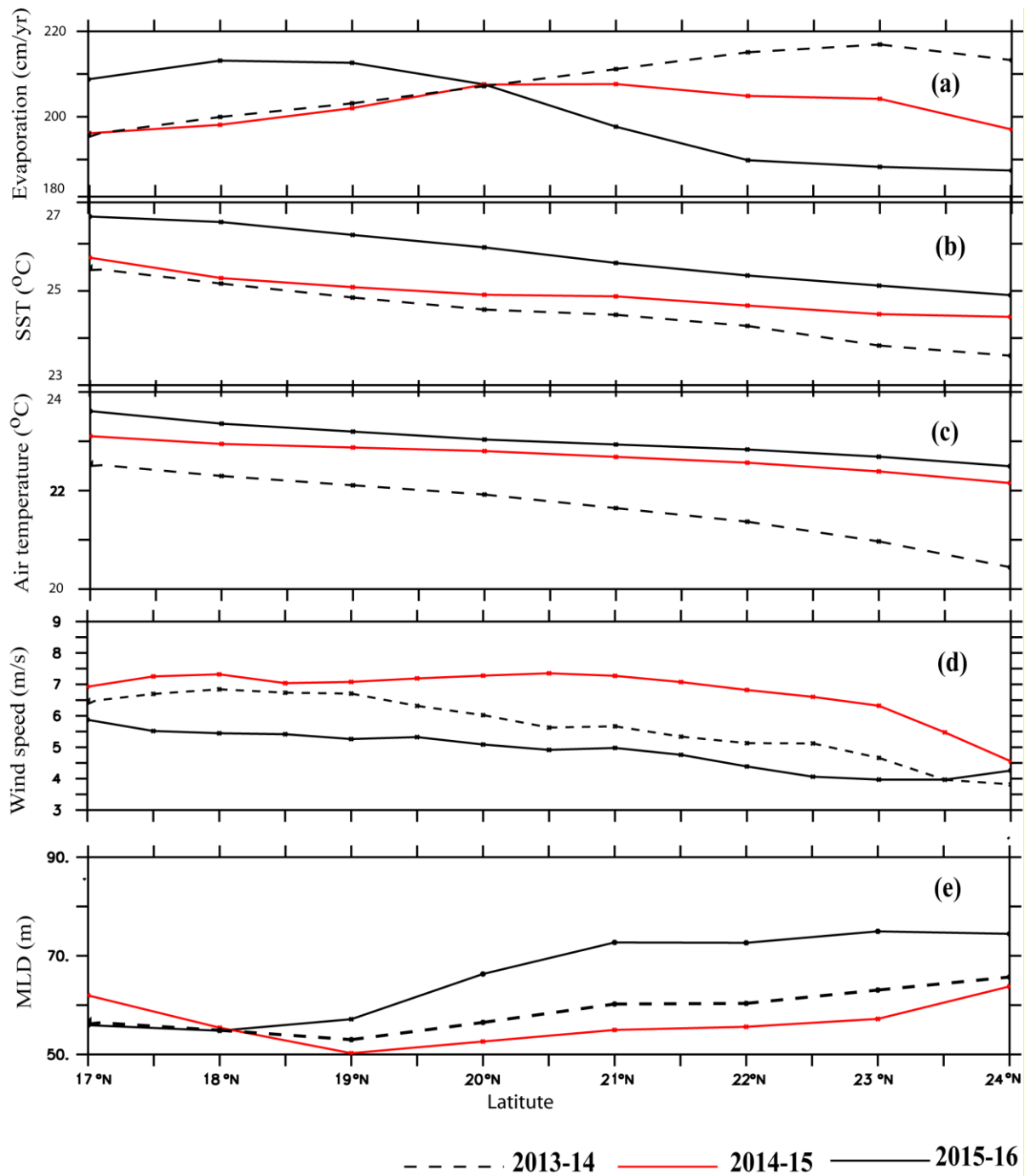


**Figure 3** Latitudinal variations (63–69°E averaged) in (a) Evaporation ( $\text{cm yr}^{-1}$ ); (b) sea surface temperature (SST; in  $^{\circ}\text{C}$ ), (c) Air temperature ( $^{\circ}\text{C}$ ), (d) Wind speed (m/s) and (e) Mixed Layer Depth (MLD in m) during December 2013–February 2014 (black dash line), December 2014–February 2015 (red line) and December 2015–February 2016 (black line).

Consistent with the changes in the intensity of the atmospheric convection, the temperature in the upper oceanic water column also showed temporal variability (Figure 4). We used shoaling of the  $26^{\circ}\text{C}$  isotherm as a proxy (as it reaches the surface during the winter) for the intensity of the cooling/convection to define the extent of winter mixing on a temporal scale. During the winter

period of 2013–14 and 2014–15, the mixing was observed between the end of December and the middle of March (Figures 4a & 4b; based on the 26°C isotherm). But, during the 2015–16 ENSO, mixing occurred only for a short period from January to the end of February (Figure 4c). It indicates that the oceanic water column also responded to the intensity of the atmospheric convection. The deepening of the ML is assumed to be directly linked to the intensity of the convection/cooling and the amplitude of the bloom (Prasanna Kumar et al., 2001; Marra and Barber, 2005). Corresponding to the intensity of the winter convection during 2013–14, the ML deepened to 110m, while it was only 70m during 2014–15. Though the intensity of the convection was weak during the 2015–16 ENSO, the ML showed a maximum value of 120m (Figure 5a), which was unexpected. This deepening of ML has been analyzed in the context of warm core (anti-cyclonic) eddies in the convective region of the NEAS.

Spatial maps of sea level anomaly showed positive values in all three years (November) in the NEAS (Figure 6). Positive SLA indicates the presence of warm-core eddies and negative SLA indicates the presence of cold-core eddies (Vidya and Prasanna Kumar, 2013). Cold-core eddies upwell the nutrients to the euphotic zone through eddy-driven upwelling and enhance Chla production; while warm-core eddies suppress the availability of nutrients in the euphotic zone and reduce Chla production by pushing the nutracline downwards via eddy-driven downwelling. Figure 6 shows the presence of a warm-core eddy (positive SLA) in the vicinity of the winter convective region (black rectangle). In fact the presence of a warm-core eddy deepened the ML during 2015–2016. During a normal winter, the atmospheric driven convection through air-sea heat exchange is more prevalent than the eddy kinetic energy and the deepening of the ML is mainly controlled by the convection rather than eddy dynamics (Fischer et al., 2002). Consistent with the study by Fischer et al. (2002), the present study also did not find the deepening of the ML directly linked to the eddy dynamics during the winters of 2013–14 and 2014–15; instead, it showed a direct link with the intensity of the atmospheric convection. However, this mechanism was not favoured during the ENSO year of 2015–16. Though the intensity of the winter convection was weak during 2015–16, the deepening of the ML was reinforced by the presence of a warm-core eddy. The intensity of the warm-core eddy was comparatively stronger in 2015–16 than during the other two years (Figure 5b). This indicates that during the normal years (2013–14 and 2014–15), the eddy signal is capped (convective cooling overshoots the eddy processes) by the strong convection. However, during the 2015-16 ENSO event, the intensity of the convection decreased. As a result, eddy mixing overshoot the winter convective mixing and controlled the ML dynamics. The warm-core eddy induced downwelling during the 2015-16 ENSO event, pushed the thermocline/nutracline further downwards

and deepened the ML, thus making it more difficult for vertical mixing to reach depths where nutrients are available. The present study shows that apart from the winter convective mixing, the warm-core eddy (during ENSO 2015-16) also played a dominant role in the deepening of the ML which in turn can affect the *Chla* biomass.

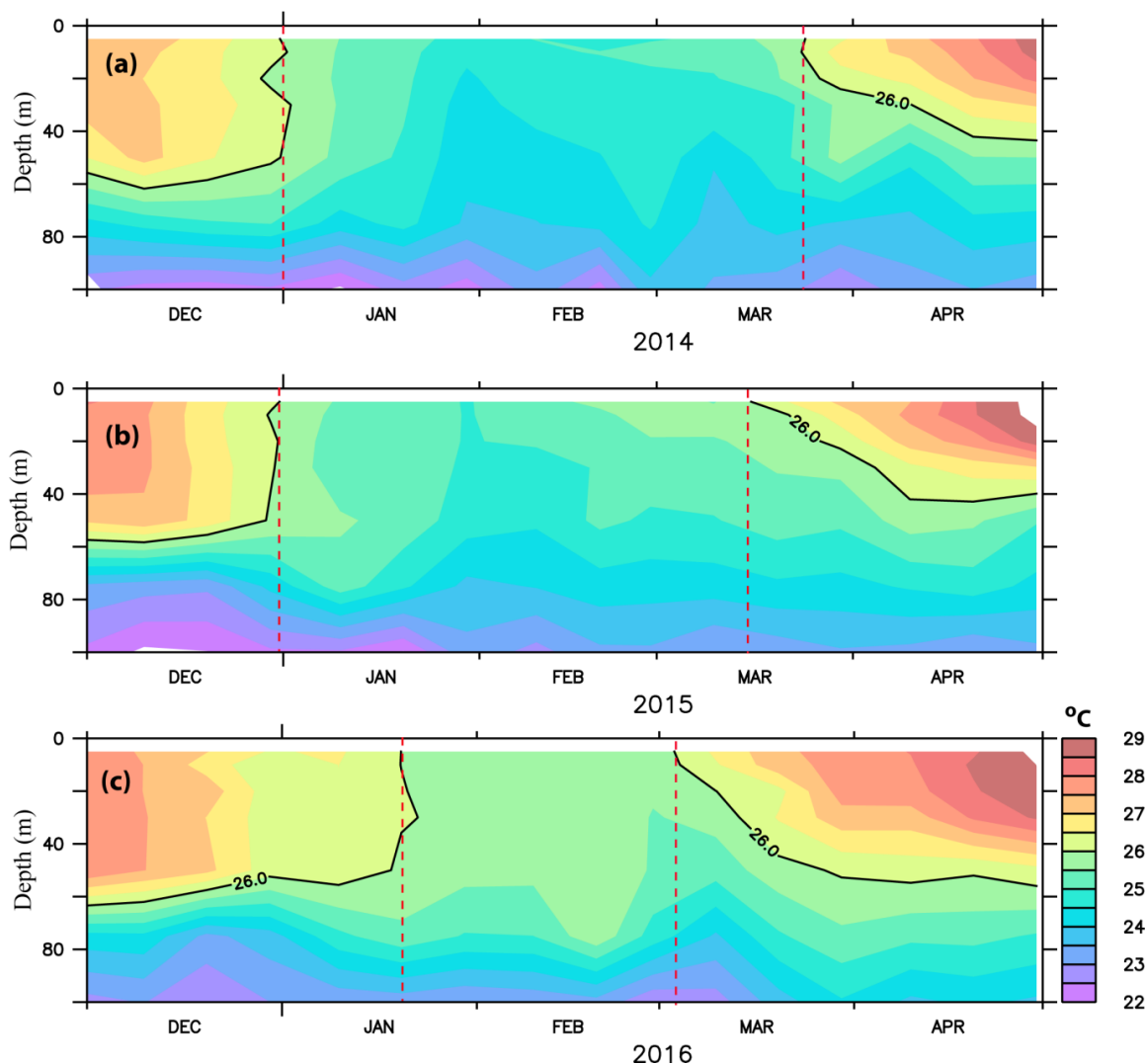


**Figure 4** Vertical structure of temperature in the upper 100m water column depicting the winter convection/cooling in the Arabian Sea during (a) December 2013–April 2014, (b) December 2014–April 2015 and (c) December 2015–April 2016. The data is averaged over the region 63–69°E and 17–24°N.

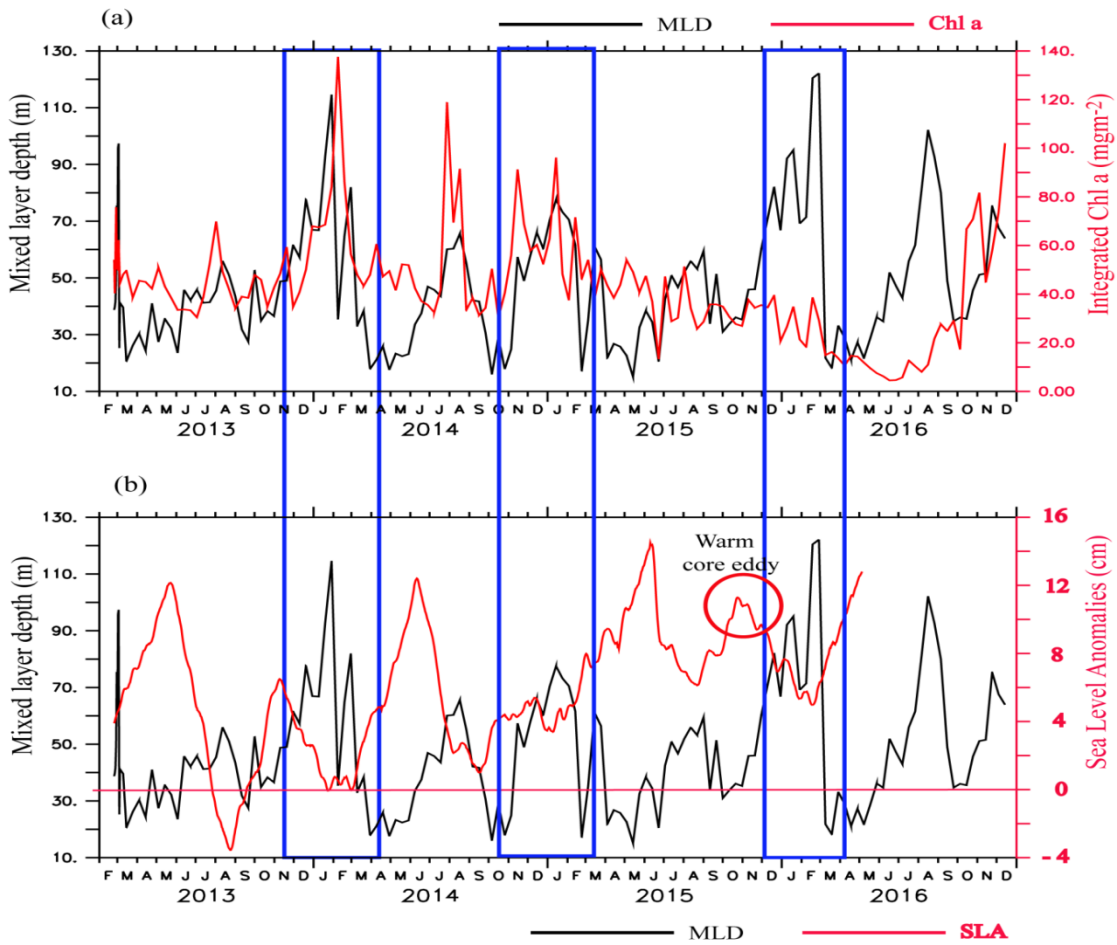


**Figure 5(a)** Time series of mixed layer depth (black line) and integrated Chl a (red line) in the upper 200m water column from the Bio-Argo, (b) Time series of mixed layer depth (black line) and sea level anomalies in the northeastern Arabian Sea (63–69°E & 17–22°N). The blue boxes represent the winter (December–February).

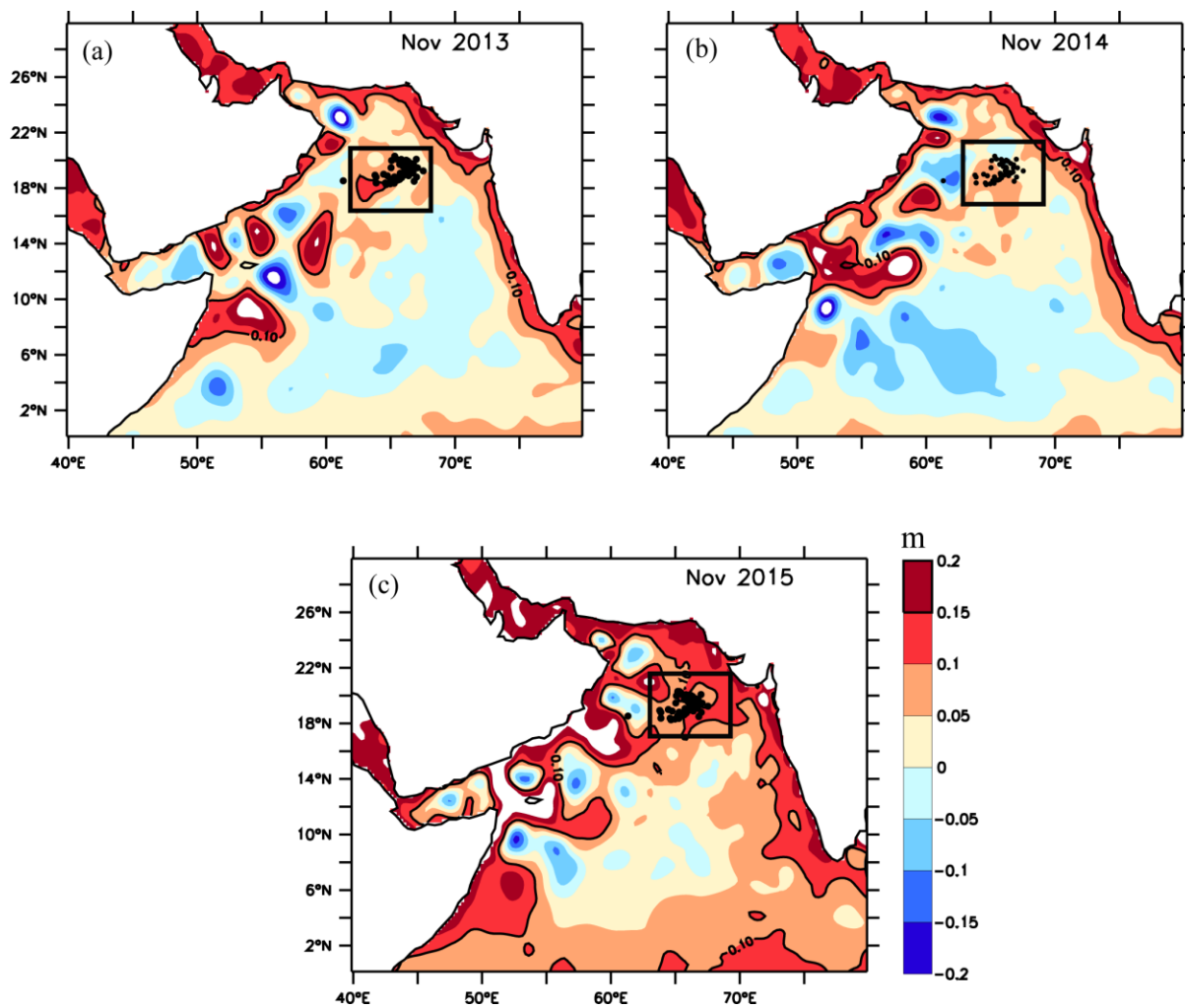


**Figure 6** Spatial maps of Sea Level Anomaly during (a) 2013 November, (b) 2014 November and (c), 2015 November. Black solid circles represent the track of Bio-Argo float (WMO ID- 2902092). The black rectangle represents the winter convective region.

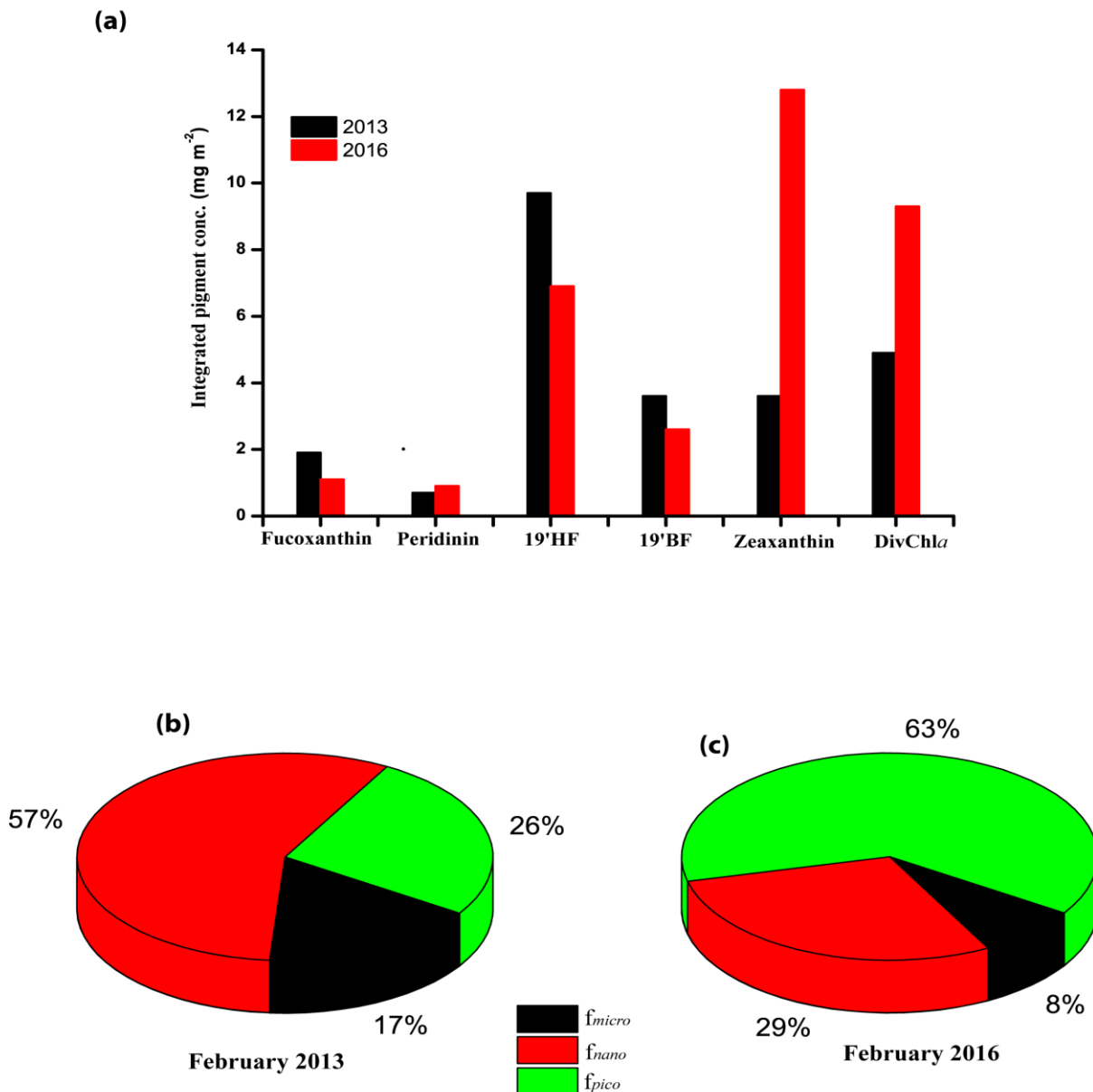


**Figure 7**(a) Depth integrated (0–50m) pigment concentrations ( $\text{mgm}^{-2}$ ) and size fractionated phytoplankton composition (%) during; (b) 08 February 2013 and (c) 02 February 2016.

Though both the processes (convective mixing and warm-core eddy) deepen the ML, changes in the prevailing physical conditions alter the nutrient availability which in turn may affect the phytoplankton community structure (the phytoplankton composition mainly depends upon the availability of nutrients in the euphotic zone). Based on the photosynthetic pigment concentrations, we further explored the impact of the 2015–16 ENSO on the phytoplankton community composition in the NEAS (Figure 7). Two years of phytoplankton pigment data collected during 8<sup>th</sup> February 2013 (normal year) and 2<sup>nd</sup> February 2016 (ENSO year) were compared (Figure 7a) in this study. Photosynthetic pigments are commonly used to understand the phytoplankton composition, as these have chemotaxonomic association. Fucoxanthin is a marker pigment for diatoms, and peridinin

usually indicates the presence of dinoflagellates, both representing microplankton. 19'HF and 19'BF represent prymnesiophytes and chrysophytes, respectively (nanoplankton). Zeaxanthin represents *Synechococcus*, whereas divinyl chlorophyll-*a* (DivChl*a*) and DivChl*b* are the marker pigments for *Prochlorococcus* (both representing picoplankton).

Microplankton pigments were compared between the normal year (2013) and ENSO year (2016) to understand the impact of the 2015-16 ENSO on the phytoplankton community structure. Integrated fucoxanthin and peridinin concentrations in the upper 50m showed a reduction in 2016 compared to 2013 (Figure 7a). Size fractionated analysis of phytoplankton showed an average of 17% contribution by microplankton ( $f_{micro}$ ) during 2013 which reduced to 8% during 2016 (Figure 7b). This indicates that microplankton (mainly diatoms and dinoflagellates) showed a 50% reduction in their abundance during the ENSO event. Nanoplankton marker pigments (19'HF and 19'BF) also showed a reduction during 2016 (Figure 7a) which reflected a 50% reduction in  $f_{nano}$  (57% in 2013 to 29% in 2016) during the ENSO event (Figure 7b & 7c). In contrast, picoplankton contribution to the total phytoplankton ( $f_{pico}$ ) doubled (26% in 2013 increased to 63% in 2016) during the ENSO event (Figure 7b & 7c). Integrated zeaxanthin and DivChl*a* concentrations were higher in 2016 compared to 2013 (Figure 7a). Matsumoto et al. (2004) showed that ENSO fluctuation could influence the picophytoplankton variability and their new production in the central and western equatorial Pacific. Among the picophytoplankton, the ENSO-driven shifts of water mass resulted in an eastward extension of *Prochlorococcus* and *Synechococcus*, and westward development of picoeukaryotes in the equatorial Pacific (Matsumoto et al. 2004). Results of the present study also showed a shift in the phytoplankton community during the 2016 winter in response to the 2015 ENSO event. A reduction in microplankton and nanoplankton abundance was associated with an increased abundance in the picoplankton community, mainly contributed by *Synechococcus* and *Prochlorococcus*. Masotti et al. (2011) also showed a large-scale shift in phytoplankton groups in the Equatorial Pacific during ENSO cycles. These results from the other basins are in line with the inference of this study.

#### 4. Conclusion

The present study explores the impact of the 2015-16 ENSO on the winter phytoplankton bloom in the northeastern Arabian Sea. During a normal winter, convective cooling deepens the ML, which in turn increases vertical mixing of nutrients to the euphotic zone. During ENSO (as seen in 2015-16), the intensity of the winter convection was weaker than normal, leading to weakening of convective



mixing in the following winter. Further, during the 2015-16 ENSO event, a downwelling event caused by a warm-core eddy increased the depth of the mixed layer, but pushed the nutricline further downwards and restricted the nutrient availability to the euphotic zone. Though both the processes deepen the ML, changes in the prevailing physical conditions alter the nutrient availability, which in turn affects the phytoplankton community structure. The 50% reduction in Chl $a$  concentration in the NEAS in February 2016 compared to normal years is associated with the 2015-2016 ENSO event. Also, phytoplankton marker pigments showed a 50% reduction in microplankton abundance, along with increased abundance in picoplankton during 2016 compared to a normal year (2013). Hence, the present study clearly delineates the impact of ENSO on phytoplankton composition in the NEAS.

### **Acknowledgments:**

Authors thank the Director, CSIR-National Institute of Oceanography and Council of Scientific and Industrial Research (CSIR), New Delhi for all support and encouragement. We express our gratitude to Dr. Paul Guard, BMT, Brisbane, Australia for meticulously going through the manuscript and suggesting the English corrections. We sincerely thank the Editor Alberto Piola and the anonymous reviewer for his/her critical review and suggestions to improve the quality of the manuscript. We are also thankful to the chief scientists and participants of *R.V. Sindhu Sankalp* during the SSK-46 and SSK-87 cruises. Mr. Chndrasekhararao is acknowledged for his help in pigment analysis. PJV acknowledges DST-SERB for the fast track young scientist fellowship. SK acknowledges CSIR (INDIAS-IDEA) and Ministry of Earth Sciences (SIBER-INDIA) for the financial support. Details of the data sets used are mentioned in the data and methods section. The NIO contribution number is xxxx

### **References:**

- Al-Naimi, N., Raitsos, D.E., Ben-Hamadou, R., Soliman, Y., 2017. Evaluation of Satellite Retrievals of Chlorophyll-*a* in the Arabian Gulf. *Remote Sens.* 9, 301.
- Banse, K., 1968. Hydrography of the Arabian Sea shelf of India and Pakistan and effects on demersal fishes. *Deep Sea Res. Oceanogr. Abstr.* 15, 45–79.
- Banse, K., 1987. Seasonality of phytoplankton chlorophyll in the central and northern Arabian Sea. *Deep Sea Res., Part A.* 34, 713–723.
- Banse, K., and D.C. English., 1993. Revision of satellite-based phytoplankton pigment data from the Arabian Sea during the Northeast Monsoon. *Marine Research (Pakistan)*. 2, 83-103.
- Banse, K., and C.R. McClain., 1986. Winter blooms of phytoplankton in the Arabian Sea as observed by the Coastal Zone Color Scanner. *Marine Ecology Progress Series*, 34, 201-211.

- Bauer, S., Hitchcock, G. L., Olson, D.B., 1991. Influence of monsoonally-forced Ekman dynamics upon surface layer depth and plankton biomass distribution in the Arabian Sea. *Deep Sea Res., Part .* 38, 531-553.
- Brock, J. C., McClaim, C. R., Hay W. W., 1992. A south-west monsoon hydrographic climatology for the northern Arabian Sea. *J. Geophys. Res.* 97, 9455-9465.
- Catherine,S , Virginie, T ., the Bio Argo Team., 2015. Argo Quality Control Manual For Biogeochemical Data. <http://dx.doi.org/10.13155/40879>.
- Currie, J. C., Lengaigne, M., Vialard, J., Kaplan, D. M., Aumont, O., Naqvi, S. W. A., Maury, O., 2013. Indian Ocean Dipole and El Niño/Southern Oscillation impacts on regional Chl-a anomalies in the Indian Ocean. *Biogeosciences.* 10, 6677-6698, doi:10.5194/bg-10-6677-2013.
- Dickey,T.D., Marra, J., Sigurdson, D.E., Weller, R.A. , Kinkade, C.S., Zedler, S.E. et al.,1998. Seasonal variability of bio-optical and physical properties in the Arabian Sea: October 1994–October 1995. *Deep-Sea Research II.* 45, 2001-2025.
- Findlater, J. 1969. A major low-level air current near Indian Ocean during northern summer. *Q. J. Roy. Meteorol. Soc.* 95, 362-&.
- Fischer, A. S., Weller, R. A., Rudnick, D. L., Eriksen, C. C., Lee, C. M., Brink, K. H., Fox, C. A., Leben R. R., 2002. Mesoscale eddies, coastal upwelling, and the upper-ocean heat budget in the Arabian Sea. *Deep Sea Res. Part II.* 49, 2231–2264.
- Garrison, D.L., Gowing, M.M., Hughes,M.P., Campbell, L, Caron D.A., Dennett, M.R., Shalapyonok, A, Olson, R.J., Landry, M.R., Brown,S.L., Liu H., Azam, F., Steward, G.F., Ducklow, H.W., Smith, D.C., 2000. Microbial food web structure in the Arabian Sea: a US JGOFS study. *Deep-Sea Res. II.* 47, 1387-1422.
- Gundersen, J.S., Gardner, W.D., Richardson, M.J., Walsh, I.D., 1998. Effects of monsoons on the temporal and spatial variations of particulate matter and chlorophyll in the Arabian Sea. *Deep-Sea Research II.* 45, pp. 2103-2132.
- Keerthi, M.G., Lengaigne, M., Levy, M., Vialard, J., Parvathi, V., De Boyer Montégut, C., Ethé, C., Aumont, O., Suresh, I., Akhil, V.P., Muraleedharan, P.M., 2017. Physical control of interannual variations of the winter chlorophyll bloom in the northern Arabian Sea. *Biogeosciences.* 14, 3615–3632. <https://doi.org/10.5194/bg-14-3615-2017>.
- Koné, V., Aumont, A., Lévy, M., and Resplandy, L., 2009. Physical and biogeochemical controls of the phytoplankton seasonal cycle in the Indian Ocean: A modeling study, *Geoph. Monog. Series.* 185, 147–166, doi:10.1029/2008GM000700.
- Kurian, S., Roy, R., Repeta, D. J., Gauns, M., Shenoy, D. M., Suresh, T., Sarkar, A., Narvenkar, G., Johnson, C. G., Naqvi, S. W. A., 2012. Seasonal occurrence of anoxygenic photosynthesis in Tillari and Selaulim reservoirs, Western India. *Biogeosciences.* 9(7), 2485–2495, doi:10.5194/bg-9-2485-2012.

- Lévy, M., Shankar, D., André, J.-M., Shenoi, S. S. C., Durand, F., de Boyer Montégut C., 2007. Basin-wide seasonal evolution of the Indian Ocean's phytoplankton blooms. *J. Geophys. Res.* 112, C12014, doi:[10.1029/2007JC004090](https://doi.org/10.1029/2007JC004090).
- Madhupratap, M., Kumar, S. P., Bhattathiri, P. M. A., Kumar, M. D., Raghukumar, S., Nair, K. K. C., Ramaiah, N., 1996. Mechanism of the biological response to winter cooling in the northeastern Arabian Sea. *Nature*. 384, 549–552.
- Marra, J., Barber, R. T., 2005. Primary productivity in the Arabian Sea: A synthesis of JGOFS data. *Prog. Oceanogr.* 65,159–175.
- Matsumoto, K., Furuya, K., Kawano, T., 2004. Association of picophytoplankton distribution with ENSO events in the equatorial Pacific between 145°E and 160°W. *Deep-Sea Research I*. 51, 1851–1871.
- Masotti, I., Moulin, C., Alvain, S., Bopp, L., Tagliabue, A., and Antoine, D., 2011. Large-scale shifts in phytoplankton groups in the Equatorial Pacific during ENSO cycles. *Biogeosciences*. 8, 539–550.
- McCreary, J.P., Murtugudde, R., Vialard, J., Vinayachandran, P.N., Wiggert, J.D., Hood, R.R.,, Shankar, D., Shetye, S., 2009. Biophysical processes in the Indian Ocean. *Indian Ocean Biogeochemical Processes and Ecological Variability*. pp.9- 32.
- McPhaden, M. J., Zebiak, S. E., Glantz, M. H., 2006. ENSO as an integrating concept in Earth science. *Science*. 314, 1740–1745, doi:[10.1126/science.1132588](https://doi.org/10.1126/science.1132588).
- Murtugudde, R., Busalacchi, A. J., 1999. Interannual variability of the dynamics and thermodynamics of the tropical Indian Ocean. *J. Climate*. 12, 2300–2326.
- Murtugudde, R., McCreary, J. P., Busalacchi, A. J., 2000. Oceanic processes associated with anomalous events in the Indian Ocean with relevance to 1997 –1998. *J. Geophys. Res.* 105, 3295–3306.
- Prakash, S., Ramesh, R., 2007. Is the Arabian Sea getting more productive?. *Curr. Sci.* 92, 667–671.
- Prasanna Kumar, S., Prasad, T. G., 1996. Winter cooling in the Arabian Sea, *Curr. Sci.* 71, 834–841.
- Prasanna Kumar, S., Ramaiah, N., Gauns, M., Sarma, V., Muraleedharan, P.M., Raghukumar, S., Kumar, M.D., Madhupratap, M., 2001. Physical forcing of biological productivity in the northern Arabian Sea during the Northeast Monsoon. *Deep-Sea Res. II*. 48, 1115–1126.
- Saji, N. H., Goswami, B. N., Vinayachandran, P. N., Yamagata. T., 1999. A dipole mode in the tropical Indian Ocean. *Nature*. 401, 360–363.
- Sarma, V. V. S. S., 2006. The influence of Indian Ocean Dipole (IOD) on biogeochemistry of carbon in the Arabian Sea during 1997–1998. *J. Earth Syst. Sci.* 115, 433–450.
- Sawant, S., Madhupratap, M., 1996. Seasonality and composition of phytoplankton in the Arabian Sea. *Curr.Sci.* 71, 869-873.

Schott F.A., McCreary J. P., 2001. The monsoon circulation of the Indian Ocean, *Prog Oceanogr.* 51, 1–123

Tarran, G.A., Burkill, P.H., Edwards, E.S., Woodward, E.M.S., 1999. Phytoplankton community structure in the Arabian Sea during and after the SW monsoon, 1994 *Deep-Sea Research II.* 46 (1999), pp. 655-676.

Trenberth, K. E.T. J. Hoar., 1997. El Niño and climate change. *Geophys. Res. Lett.* 24, 3057–3060.

Uitz, J., Claustre, H., Morel, A., Hooker, S. B., 2006. Vertical distribution of phytoplankton communities in open ocean: An assessment based on surface chlorophyll. *J. Geophys. Res.* 111, C08005, doi:10.1029/2005JC003207.

Vidya, P.J., Prasanna Kumar, S., 2013. Role of mesoscale eddies on the variability of biogenic flux in the northern and central Bay of Bengal. *J. Geophys. Res.* 118, 5760–5771. <http://dx.doi.org/10.1002/jgrc.20423>.

Vijith, V., Vinayachandran, P. N., Thushara, V., Amol, P., Shankar, D., Anil, A. C., 2016. Consequences of inhibition of mixed-layer deepening by the West India Coastal Current for winter phytoplankton bloom in the northeastern Arabian Sea. *J. Geophys. Res. Oceans*, 121, 6583–6603, doi:[10.1002/2016JC012004](https://doi.org/10.1002/2016JC012004).

Webster, P. J., Moore, A. M., Loschnigg, J. P., Leben, R.R., 1999. Coupled ocean– atmosphere dynamics in the Indian Ocean during 1997–98. *Nature.* 401, 356–360.

Wiggert, J. D., Murtugudde, R., McClain, C.R., 2002. Processes controlling interannual variations in wintertime (Northeast Monsoon) primary productivity in the central Arabian Sea. *Deep Sea Res., Part II*, 49, 2319-2343.

Wiggert, J. D., Hood, R. R. Banse, K., Kindle, J. C., 2005. Monsoon-driven biogeochemical processes in the Arabian Sea, *Prog. Oceanogr.* 65, 176–213.

Wiggert, J. D., Vialard, J., Behrenfeld, M. J., 2009. Basin-wide modification of dynamical and biogeochemical processes by the positive phase of the Indian Ocean dipole during the SeaWiFS era, in *Indian Ocean Biogeochemical Processes and Ecological Variability*. *Geophys. Monogr. Ser.*, vol. 185, edited by J. D. Wiggert et al., pp. 385–407, AGU, Washington, D. C.

Wood, A. M., Lipsen, M., Coble, P., 1999. Fluorescence-based characterization of phycoerythrin-containing cyanobacterial communities in the Arabian Sea during the Northeast and early Southwest Monsoon (1994-1995). *Deep-Sea Research II.* 46, 1769-1790.